General Disclaimer

One or more of the Following Statements may affect this Document

- This document has been reproduced from the best copy furnished by the organizational source. It is being released in the interest of making available as much information as possible.

- This document may contain data, which exceeds the sheet parameters. It was furnished in this condition by the organizational source and is the best copy available.

- This document may contain tone-on-tone or color graphs, charts and/or pictures, which have been reproduced in black and white.

- This document is paginated as submitted by the original source.

- Portions of this document are not fully legible due to the historical nature of some of the material. However, it is the best reproduction available from the original submission.

MILLIMETER WAVES STUDY

E. R. Graf, Project Leader

RADIO FREQUENCY SYSTEM

M. A. Honnell, Project Leader

MICROWAVE RESEARCH LABORATORY

NINETEENTH QUARTERLY REPORT
1 September 1968 to 1 December 1968
CONTRACT NAS8-11184

GEORGE C. MARSHALL SPACE FLIGHT CENTER
NATIONAL AERONAUTICS AND SPACE ADMINISTRATION
HUNTSVILLE, ALABAMA

ENGINEERING EXPERIMENT STATION

AUBURN UNIVERSITY

AUBURN, ALABAMA

FOREWORD

This report summarizes the progress of the Auburn University Electrical Engineering Department toward fulfillment of the requirements in NASA Contract NAS8-11184. The contract is administered by the Engineering Experiment Station. Monthly progress letters have been submitted prior to this report.

TABLE OF CONTENTS

LIST OF FIGURES

A-MILLIMETER WAVES STUDY

35 GHz Communication System Study

E. R. Graf and F. A. Ford

I. INTRODUCTION

In the design of a communication link, adequate characterization of the transmission channel is imperative. All disturbances, sources of distortion, and sources of noise must be evaluated. This characterization will aid the designer in determining power requirements, the advantages of various terminal locations, achievable bandwidth, system reliability, and component requirements. To this end, the effort during this reporting period was directed toward the description of the satellite-earth transmission channel at K_a-band. Attention was focused on amplitude variations, limitations, and distortion. The following section reports the areas studied and the results of their evaluation.

II. AMPLITUDE VARIATIONS, LIMITATIONS, AND DISTORTIONS

A. Ionospheric Attenuation

In an ionized medium, free electrons are set in motion by a propagating electromagnetic wave. Periodic forces exerted on the electrons cause them to vibrate. Absorption of energy occurs when these electrons give up energy through collisions with the heavier ions and neutral particles that are present.

If a complex refractive index, η, is assumed,

$$\eta^2 = (\mu - i\chi)^2 \tag{1}$$

where μ = the real part of η,

χ = the imaginary part of η,

and the behavior of the imaginary part, χ, dictates the amount of absorption in the medium. The absorption coefficient, κ, may be defined as [1]

$$\kappa = \frac{\omega}{c}\chi \tag{2}$$

where ω = the radian frequency of the wave,

c = the speed of light,

thus providing a measure of attenuation per unit distance.

Neglecting the earth's magnetic field, κ may be evaluated from

the Appleton-Hartree formulas [2] as follows:

$$\kappa = \frac{e^2}{2\varepsilon_o mc} \frac{1}{\mu} \frac{N\nu}{\omega^2+\nu^2} \tag{3}$$

where e = the charge on an electron,

ε_o = the permittivity of free space,

m = the mass of an electron,

N = the electron number density,

ν = the angular collision frequency of the electrons.

This absorption may be mathematically classed as deviative or non-deviative. Non-deviative absorption implies $\mu \approx 1$ and the product $N\nu$ large. Deviative absorption occurs as μ approaches zero.

With $\omega = 2\pi(35 \times 10^9)$, $\omega >> \nu$ and the conditions for non-deviative absorption are met. From (3), it may be observed that losses are inversely proportional to the square of the frequency. Millman [3] has determined maximum daytime attenuation to be 1.28 dB at 100 MHz. This figure implies losses of 10^{-5} dB at K_a-band.

With such a low level of absorption, variations in this figure due to diurnal changes, seasonal changes, and winter anomally, (a middle-latitude seasonal phenomena of increased absorption), are of no consequence. The effects of solar flare absorption events, auroral absorption events, and polar-cap absorption events may be approximated by assuming that each varies inversely as the square of frequency [4]. This method of approximation being accepted, calculations based on measured data at lower frequencies may be carried out. These calculations show absorption due to the phenomena above to be negligibly small, also.

B. Tropospheric Attenuation

Clear-weather absorption

The constituent gases of the troposphere are responsible for the attenuation of the millimeter wave as it traverses this region with water vapor and oxygen having by far the greatest effect in the EHF portion of the spectrum. Several other gases possess highly absorptive characteristics at these frequencies, but because of their low molecular densities they contribute insignificantly to overall attenuation.

The coupling of energy from a passing wave to gaseous molecules is attributable to the dipole moments of the substances. Water vapor possesses a strong electric moment while oxygen, being paramagnetic, has associated with it a magnetic moment. Both molecules have numerous possible modes of rotation and vibration correspondent to each of which is a discreet energy level. Every transition from one energy level to another may be related to a frequency.

Excited by the passing wave, a gas molecule experiences a transition to a higher energy level and a new dynamic mode with the specific transition being determined by the frequency of the wave. An amount of energy equal to the change in energy level of the molecule is then transferred from the wave and an attenuative effect is observed.

Straiton and Tolbert [5] have published measured values of attenuation due to water vapor at five elevations. These data are shown in Fig. 1. Computations from these data yield a value of 0.0273 dB/km in a vertical column from sea level to a height of 8.5 km for a sea-level vapor density of 1 g/m^3. With the assumption that water vapor density

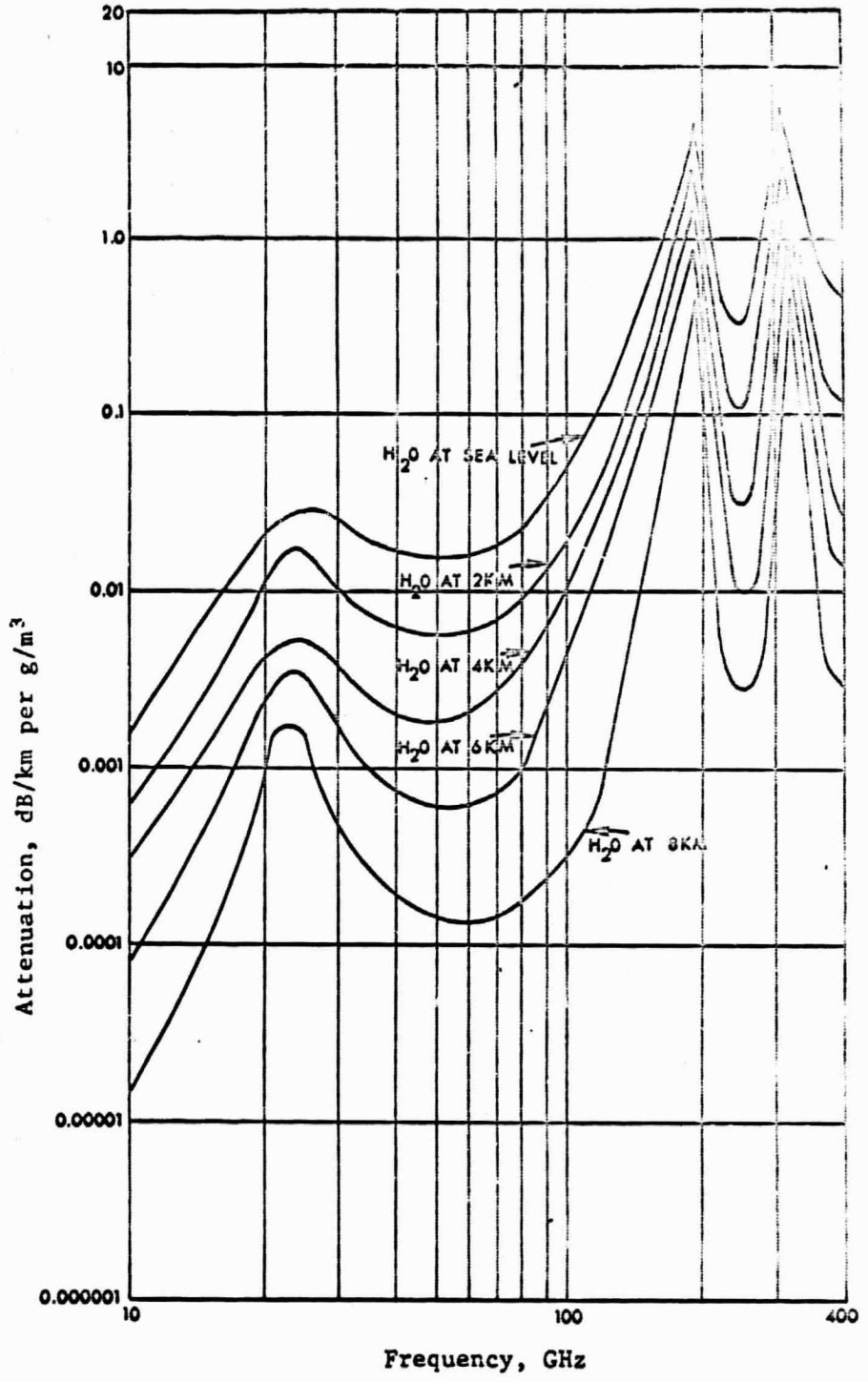

Fig. 1.--Water vapor absorption at five elevations [5].

decreases from the surface value as $e^{-0.5z}$, where z is the height in kilometers, attenuation from 8.5 km to 20 km in such a column will be 0.0004 dB. The total attenuation, then, in a 20 km column is 0.0277 dB. To find vertical attenuation for greater values of sea-level water vapor density the figure above should be multiplied by that density. Should the ground terminal be situated at an elevation appreciably above sea level, adjustments in the figures are easily made. Values of sea-level vapor density range from 1 g/m^3 to 20 g/m^3 in temperate latitudes with 7.5 g/m^3 being generally accepted as a typical figure.

Denoting sea-level vapor density by the symbol M, and the zenith angle by γ, total losses due to water vapor absorption along a practical path are represented as

$$A_{H_2O} = 0.0277(M)(\sec \gamma) \text{ dB} \qquad (4)$$

For a value of M = 7.5 g/m^3 and a zenith angle of 60°, attenuation in dB due to water vapor along the path is

$$A_{H_2O} = 0.0277(7.5)(\sec 60^\circ)$$

$$= 0.4155 \text{ dB}.$$

Classical work in the absorption of electromagnetic energy by molecular oxygen was done by Van Vleck and Weisskopf in 1945 [6] and Van Vleck in 1947 [7]. Unfortunately, the Van Vleck-Weisskopf equations contain an empirical parameter. Proper values of this constant, the so-called line-breadth constant are in doubt [8]. Experimental

measurements of oxygen losses for one-way propagation through the atmosphere have been made [9,10]. Values between 0.15 dB and 0.20 dB are indicated for zenith attenuation. The usual means for determining this loss figure is the collecting of loss data over a period of time as a function of absolute humidity and the extrapolation of these data to zero absolute humidity. The most recent suggested value obtained by this method is 0.17 dB [9].

Investigation of the Van Vleck-Weisskopf equations reveals a complicated dependence on temperature and pressure. Not only do these two parameters appear explicitly, but their effect on the aforementioned line-breadth constant is considerable.

In the absence of further experimental data and with consideration for the magnitude of other effects in the propagation path, attempting highly accurate computation of losses due to molecular oxygen seems unjustifiable.

Upcoming propagation experiments in connection with the Applications Technology Satellite (ATS) program should yield extremely valuable information in this area. Hopefully, future investigations will show that atmospheric absorption may be heuristically determined from available meteorological information, thus yielding improved accuracy with mathematically simple techniques.

As with water vapor losses, absorption losses due to oxygen along an actual propagation path may be found by multiplying zenith attenuation by the secant of the zenith angle.

Attenuation in clouds and rain

In propagating through terrestrial cloud cover, millimeter wave energy may be lost through both the mechanisms of absorption and scattering. Because the water droplets which constitute clouds are usually 10 μm or less in diameter, absorption is the more prevalent of the two.

The absorption coefficient is proportional to water content per unit volume. Observing this, one may express the total loss as

$$A_c = pMr \text{ dB} \tag{5}$$

where p = absorption of the water particles (dB/km per g/m^3)

M = water volume density (g/m^3)

r = path length through clouds (km)

Table I gives published values of the constant p.

TABLE I

PUBLISHED VALUES OF THE FACTOR p
AT 35 GHz

p dB/km per g/m^3	T °C	Source
1.10	0	Holzer, 1965 [13]
0.487	18	Goldstein, 1951 [12]
0.70	0	Mitchell, 1964 [11]
0.30	20	Mitchell, 1964 [11]

It is noted that values due to Mitchell [11] indicate a variation in the value of p that is on the order of two for a temperature variation of 20° C. Fig. 2 shows temperature correction factors (normalized to 18° C) for wavelengths of 0.5 cm and 1.25 cm from Goldstein [12]. A curve for 0.86 cm has been interpolated. From Table I and Fig. 2, a value of 0.88 dB/km per g/m^3 is taken as an average value for p at 0° C.

Values of M range from minute fractions to about 3 g/m^3 in clouds. Water content in land fogs may go up to 0.2 g/m^3, while concentrations in heavy sea fogs may exceed those in moderate rainfalls.

Holzer [13] has made useful suggestions for anticipating losses in cloud cover. Based on climatological studies, the worst enduring cloud conditions in temperate climates are those associated with a frontal zone. When such a zone is present, the area affected by cloud cover is, for present purposes, unlimited. Clouds are unbroken and extend vertically from about 2.5 km to about 6 km. A liquid water content of 0.3 g/m^3 in such clouds is to be reasonably expected.

In tropical zones, an effort to predict signal deterioration in clouds leads to the consideration of quite a different configuration. Not infrequently, cloud cover in these portions of the world consists of a heavy layer of moisture between 0.25 km and 2.75 km with less dense pillars rising to 23 km. These piller-like clouds (cumulonimbus) average 15 km in horizontal extent with separations of about 25 km. These two models, shown in Figs. 3 and 4, allow reasonable margins for attenuation in clouds to be calculated. Values for losses in fair-weather clouds fall well below those associated with the models above.

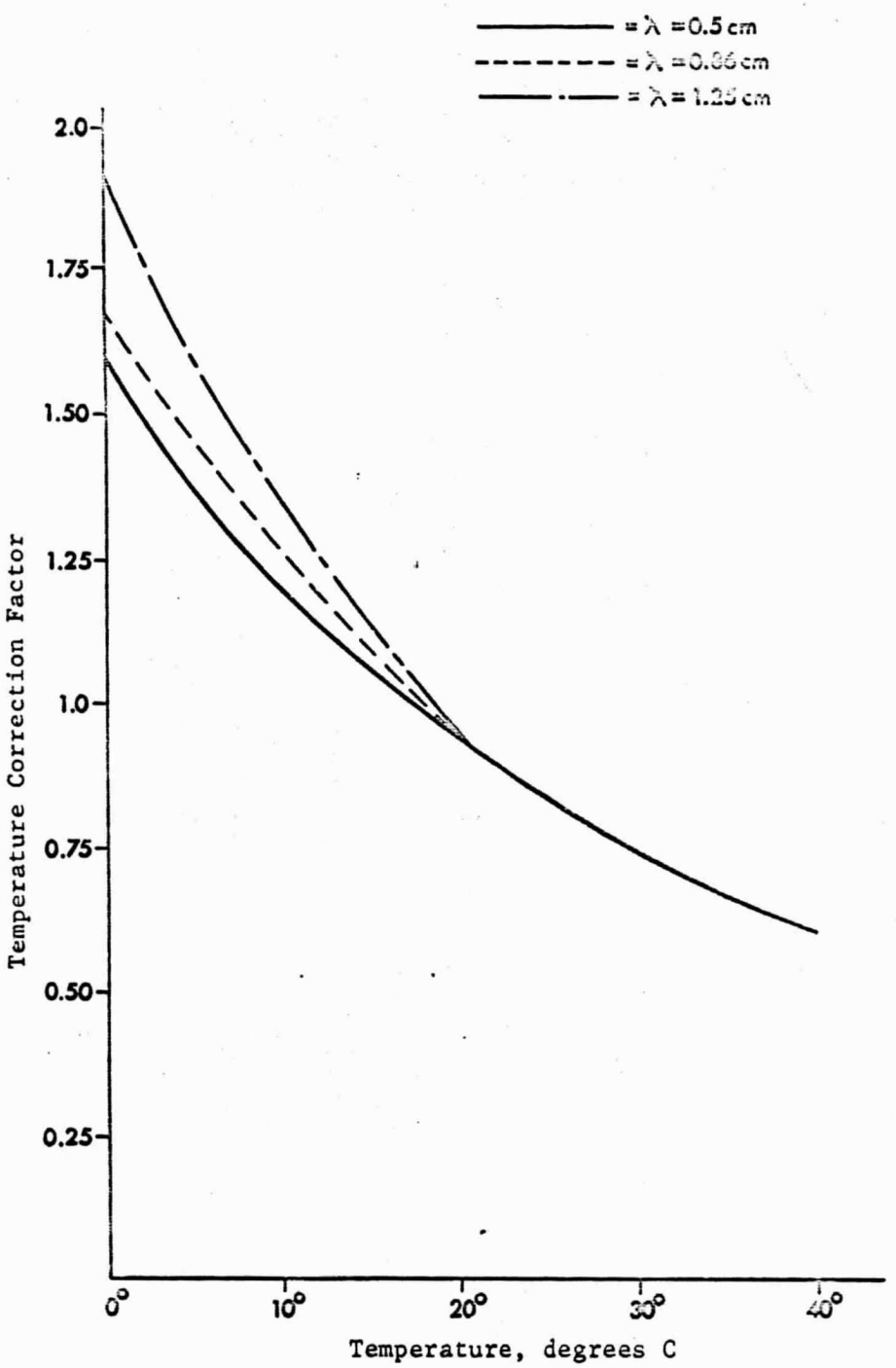

Fig. 2.--Temperature correction factors for absorption by water particles.

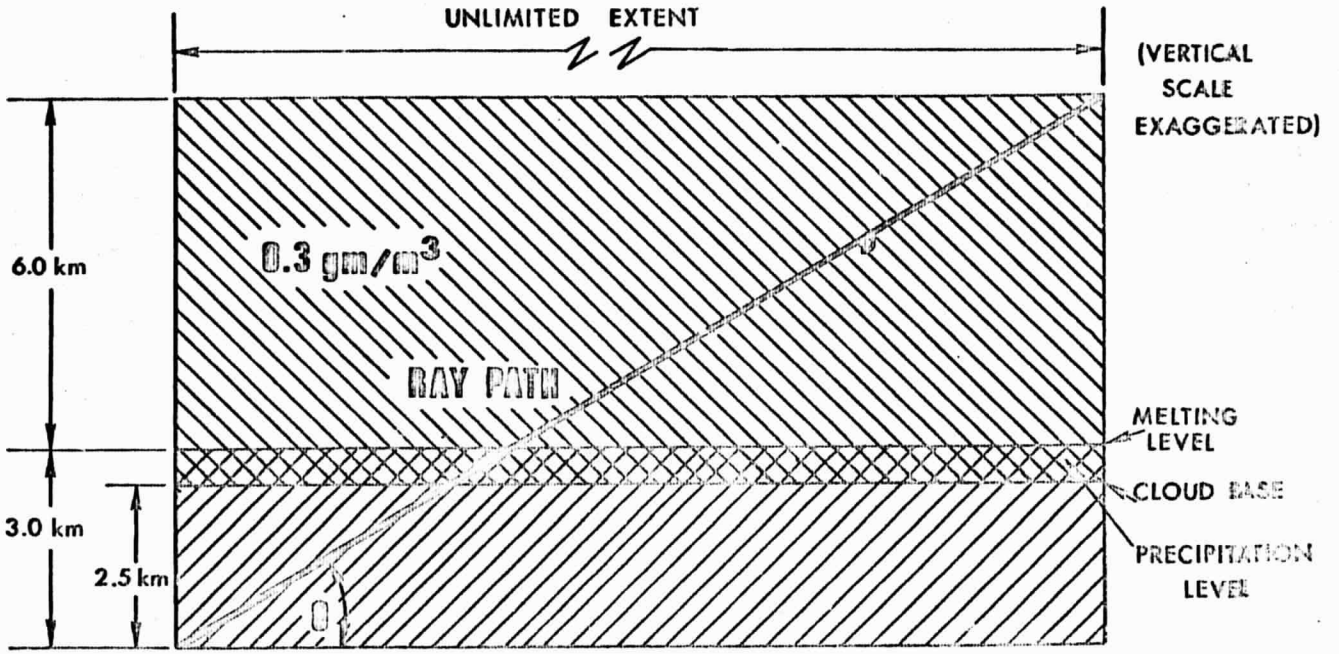

Fig. 3.--Cloud cover model for temperate latitudes [13].

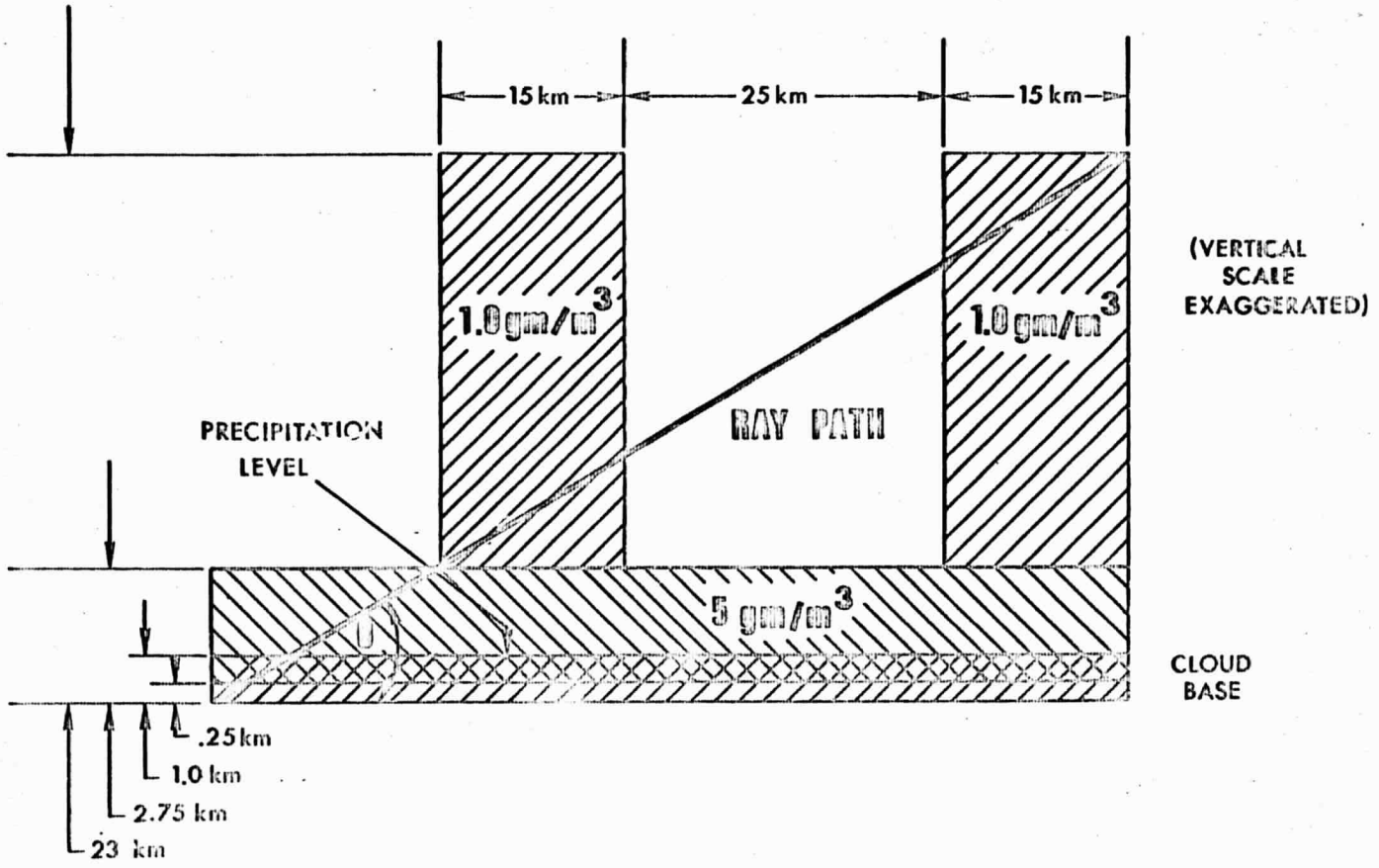

Fig. 4.---Cloud cover model for tropical latitudes.

Figures 5 and 6 show anticipated attenuation in temperate and tropical zones, respectively. In the case of the tropical model, ground terminal position was chosen so as to produce pessimistic loss figures.

The single factor that most strongly influences millimeter propagation is precipitation. At 35 GHz, losses in rain are due both to scattering and to absorption, the difference between the precipitation situation and that existing in clouds or fog being that the particles under consideration become an appreciable portion of a wavelength. In fact, raindrops sometimes attain diametrical dimensions of 0.7 cm.

The original work on the interaction of a wavefront with a spherical dielectric particle was done by Mie in 1908 [14]. Numerous investigators have made calculations based on the Mie theory. Because the magnitude of the effects are dependent on both particle size and particle number, no degree of accurate prediction is possible without detailed meteorological data. While theory is sufficient to evaluate losses in ideal rainfall configurations, experimental results have shown signal deterioration to fall well outside predicted boundaries.

The only readily available characteristic of rainfall is precipitation rate and this has been well related to drop size and number. It is generally accepted that a straight-line relationship may be established between attenuation per unit distance and precipitation rate. That is, for a given wavelength the attenuation due to precipitation, A_p, may be expressed as

$$A_p = K\rho r \text{ dB} \qquad (6)$$

where K = a constant dependent on wavelength (dB/km per mm/hr)

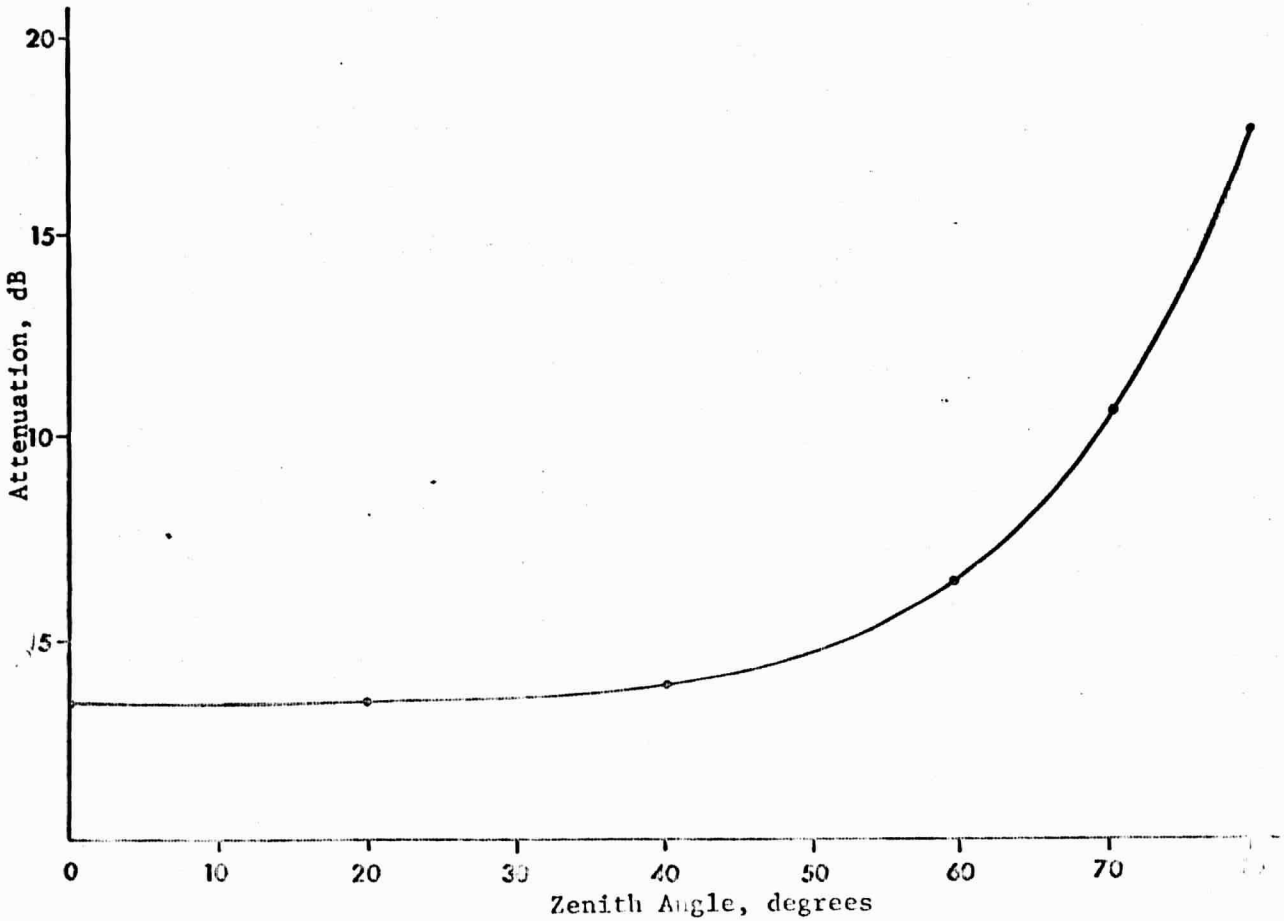

Fig. 5.--Anticipated attenuation due to temperate latitude cloud cover.

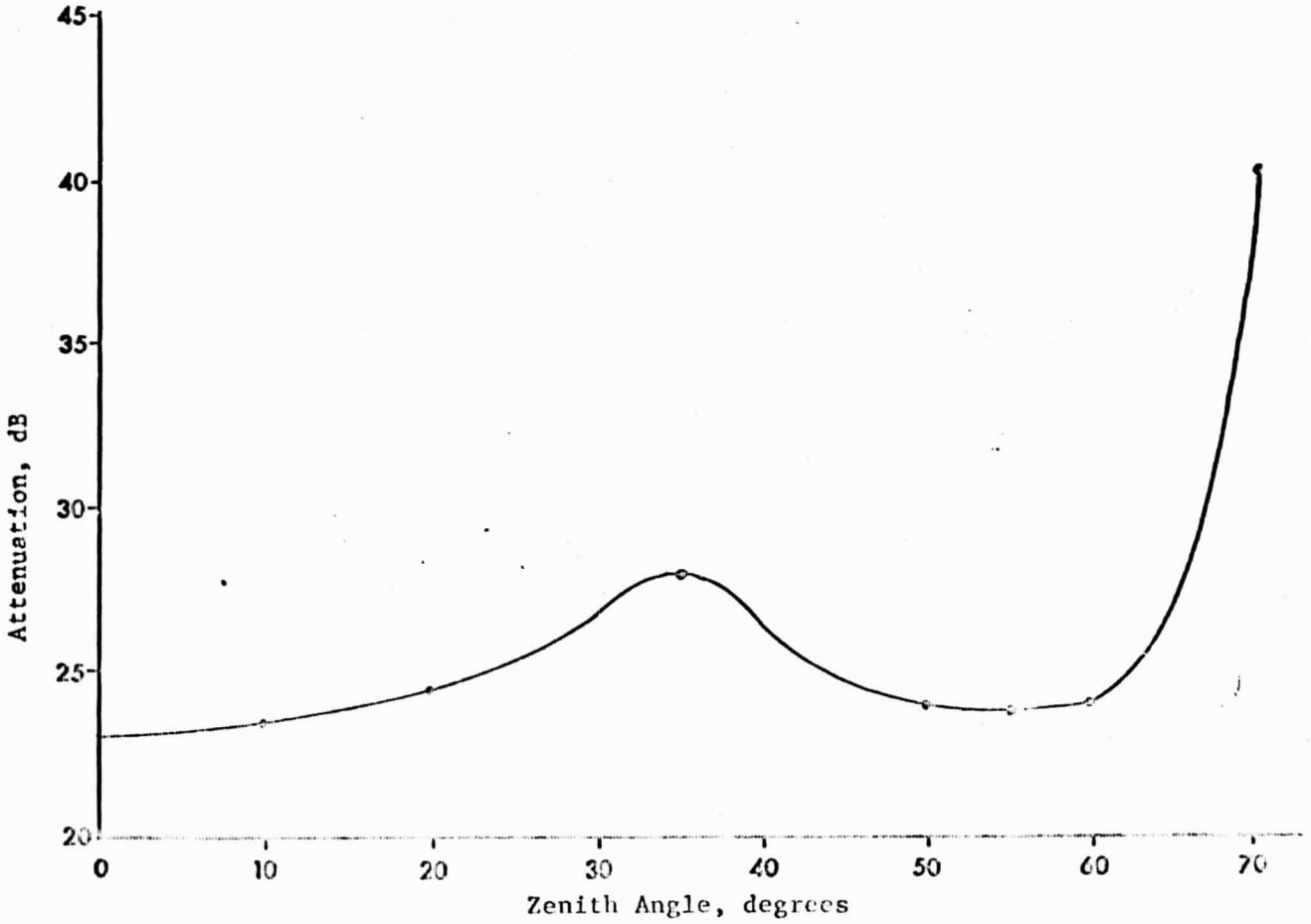

Fig. 6.--Anticipated attenuation due to tropical latitude cloud cover.

ρ = the precipitation rate (mm/hr),

r = path length through the precipitation (km).

However, several factors hinder attempts to describe a rainfall. The precipitation is by nature inhomogeneous and this condition is aggravated by the effects of wind. Also, techniques for measuring precipitation rates along the path have been inadequate in that they have provided samplings insufficient in number and considerably lagging in time the atmospheric conditions.

For the purposes of engineering design, the best data is that made available by Medhurst [15]. In his work, revised calculations on the classical basis are presented and compared to all available experimental data; disagreement is noted as quite evident and quite sizeable. Combining measured data from eleven publications, upper, lower, and mean values of the constant K are fixed. For a wavelength of 8.6 mm the values of K (dB/km per mm/hr) are:

upper - 0.52

lower - 0.15

mean - 0.40.

In this analysis, calculations will be made using Equation (6) and a value of 0.40 dB/km per mm/hr for K.

In temperate zones, precipitation begins at a height near 3 km, whereas tropical rains extend to about 1 km. Figs. 7 and 8 show A_p for vertical propagation as a function of precipitation rate. Though the slope on the curve for the tropical model is the smaller, in the

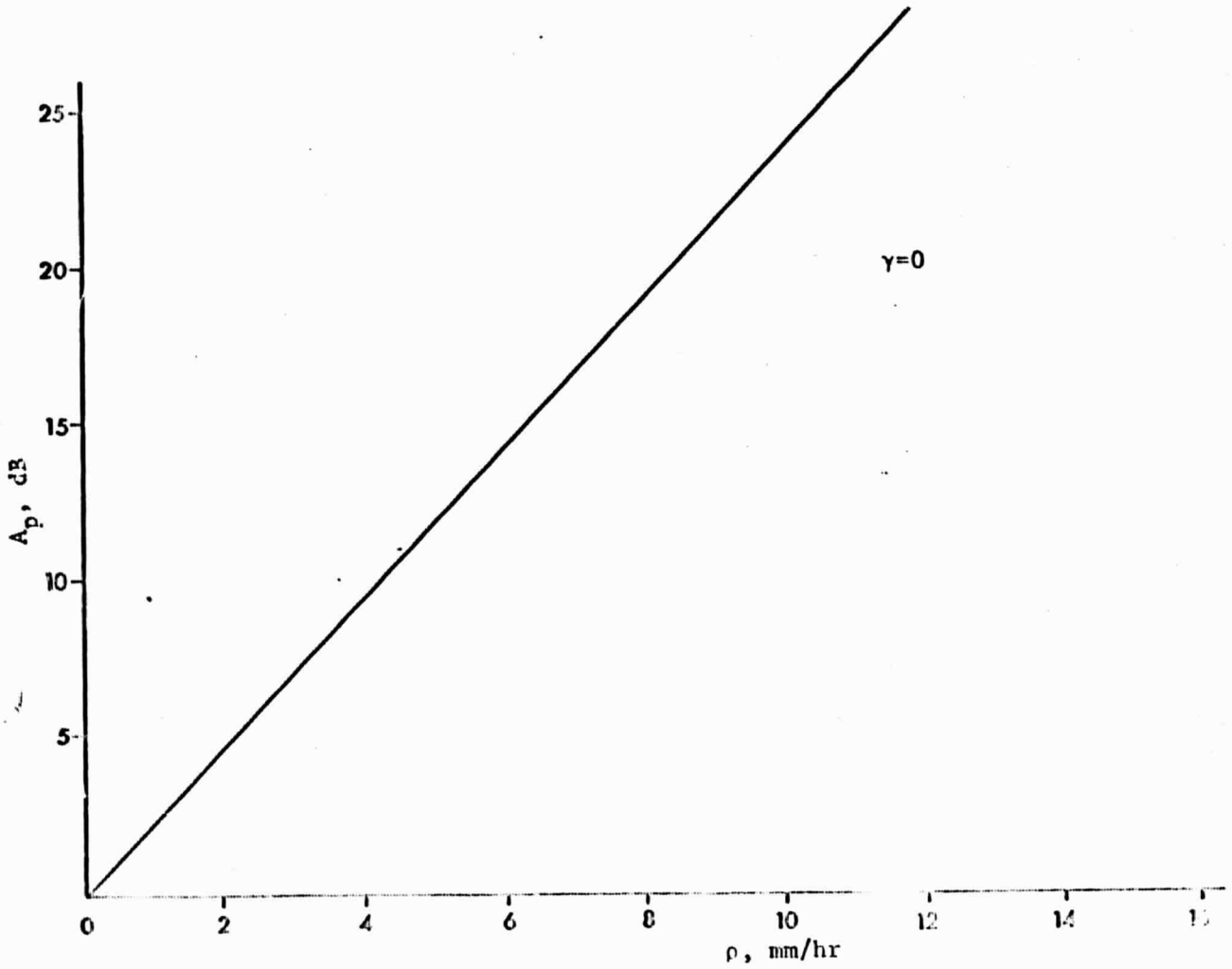

Fig. 7.--Attenuation due to precipitation in temperate latitudes.

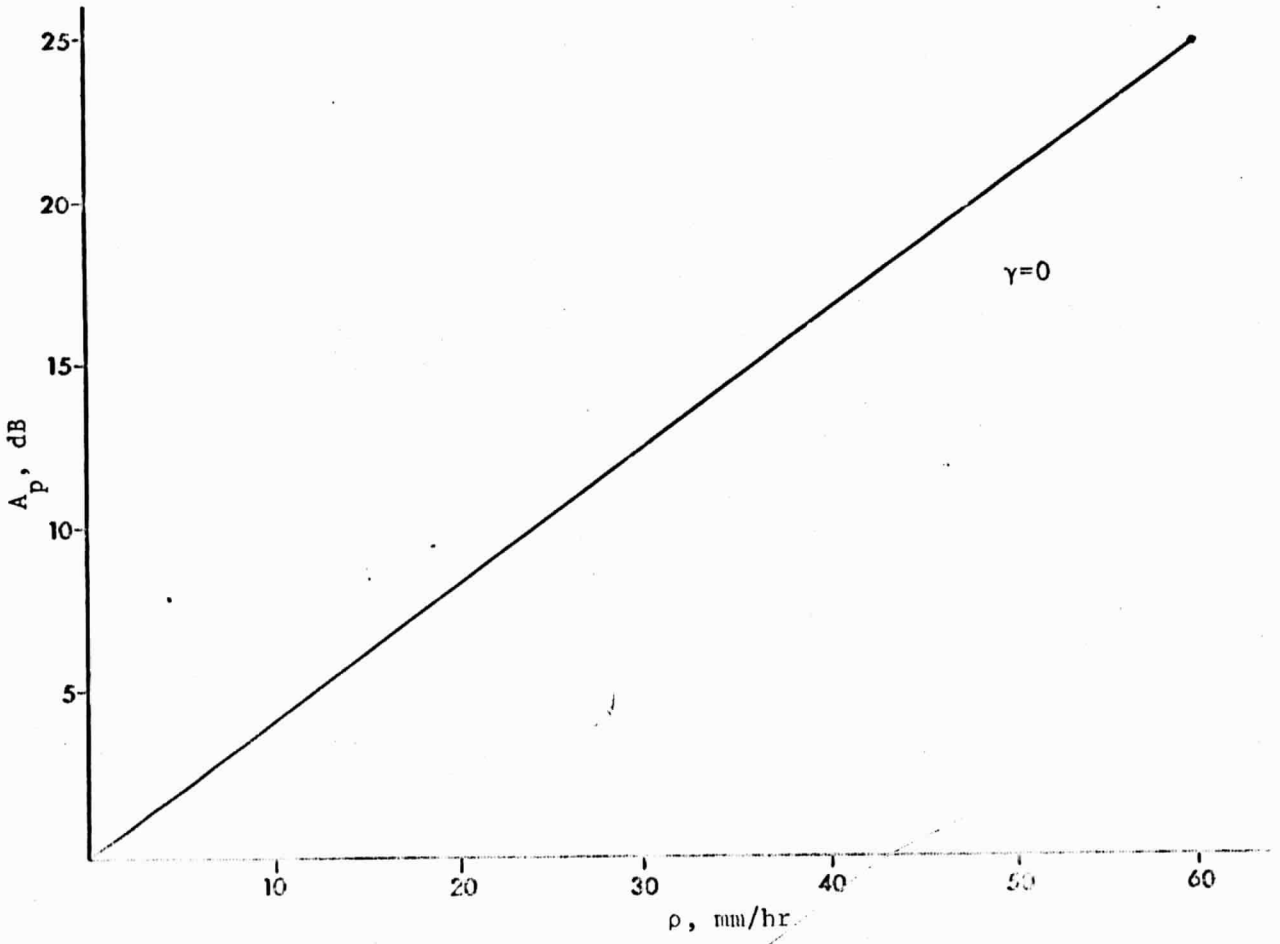

Fig. 8.--Attenuation due to precipitation in tropical latitudes.

consideration of ground terminal site the frequency and intensity of rainfall must be taken into account.

Attenuation due to ice and snow

When precipitation takes on a solid form the imaginary part of the refractive index decreases drastically. Calculations indicate attenuation due to hailstones to be in the range of 10^{-3} dB/km per stone/m^3 [12]. While attempts to measure the effects of snowfall meet with obvious difficulties, dry snow should give rise to very small values of attenuation. Moist snow, on the other hand, is expected to yield values on the order of 2.5 times those due to rainfall with the same water content [16]. This is probably due to the large concentration of particles near the precipitation level.

C. Refractive Effects

Using the Appleton-Hartree equations to describe a wave in the environment of the ionosphere, it is proper to write

$$\mu^2 = 1 - \frac{X}{1-(1/2)Y_T^2/(1-X)\pm[(1/4)Y_T^4/(1-X)^2+Y_L^2]^{1/2}} \tag{7}$$

where μ = the real part of the refractive index

$X = \omega_N^2/\omega^2$,

$Y = \omega_H/\omega$

$Y_L = \omega_L/\omega$

$Y_T = \omega_T/\omega$

ω = angular frequency of the radio wave

ω_N = angular plasma frequency = $[Ne^2/\varepsilon_o m]^{1/2}$

$\omega_T = \omega_H \sin\theta$

ω_H = angular gyro frequency of an electron

$\omega_L = \omega_H \cos\theta$

θ = the angle between wave normal and magnetic field

N = electron number density

ε_o = permittivity of free space

m = the mass of an electron

e = the charge on an electron

From this, propagation is classed as "quasi-longitudinal" or "quasi-transverse" according to the relative magnitudes of the terms under the radical in the denominator. If

$$\frac{Y_T^4}{(1-X)^2} >> 4Y_L^2 , \tag{8}$$

the class is QT (quasitransverse). If

$$\frac{Y_T^4}{(1-X)^2} << 4Y_L^2 , \tag{9}$$

the class is QL (quasi-longitudinal). As the names suggest, the two classifications correspond to approximating the angle, θ, between the wave normal and the magnetic field to be 0° (QL) or 90° (QT). This dependence on θ may be witnessed in the definitions of ω_T and ω_L.

The transitional angle, θ_c, between the two cases is given by [4]

$$\sin\theta_c \tan\theta_c = \frac{2\omega}{\omega_H} . \tag{10}$$

In the ionosphere, ω_H typically has values in the range of 10^7 rad/sec. If, then, $\omega = 2\pi(35 \times 10^9) = 2.198 \times 10^{11}$, the right side of (10)

becomes extremely large. This implies that the QL condition is satisfied for almost all cases. Now,

$$\mu^2 \simeq 1 - \frac{X}{1 \pm Y_L} \quad . \tag{11}$$

A linearly polarized wave propagating in a magnetoionic medium may be represented as the sum of two circularly polarized waves of opposite chirality. These component waves are termed the ordinary and the extraordinary waves. The value of μ obtained by assuming the plus (+) sign in (11) is associated with the ordinary wave. The smaller of the two possible values of μ, obtained by assuming the minus (-) sign, is associated with the extraordinary wave [1]. Since the two constitutive waves are presented different values of μ, they will be refracted by different amounts. The extraordinary wave will always undergo more "bending" as the real part of the refractive index associated with it deviates more from unity.

Because of this, the possibility exists that the two waves will arrive from different directions so that their respective field vectors will not be coplanar. This would represent a loss as their recombination at the ground terminal would not be perfect. Computations carried out at lower frequencies [17], where this effect would be more pronounced, indicate that millimeter propagation should not be significantly affected by this phenomena.

Because different refractive indices result in different phase velocities, it must be considered that the ordinary and extraordinary waves might traverse phase paths of different lengths. If this were the

case, the two would add at the ground terminal to give linear polarization, but with an orientation which would be other than that at the source. This, of course, is the Faraday rotation effect. The magnitude of this effect is calculated as

$$\Omega = \frac{\pi}{\lambda} \int_0^{\ell} (\mu_+ - \mu_-) d\ell = \frac{5.33 \times 10^{-5}}{\omega^2} \int_0^{\ell} N\omega_L d\ell \qquad (12)$$

where Ω = the rotation of the sum vector along the path in radians,

$d\ell$ = element of length along the propagation path,

μ_+ = the real part of the refractive index associated with the ordinary wave,

μ_- = the real part of the refractive index associated with the extraordinary wave.

Since Ω varies as ω^{-2}, results at lower frequencies may be extended to give values in the range of 5×10^{-4} radians at 35 gigahertz. Obviously, resulting losses will be negligible.

D. Fading Phenomena

Ionospheric scintillation

In satellite-earth transmissions, irregularities in ionospheric electron content often manefest themselves in a spatially varying amplitude pattern at the receiver. The effect is much the same as that of a diffraction grating and may affect communications by appearing as fading. This fading is called scintillation. The depth and frequency of this scintillation are determined by: a) relative motion between the propagation path and the inhomogenieties; b) relative positions of the transmitter, the irregular regions, and the receiver; c) the radio

frequency of the wave; d) characteristics of the inhomogenieties including their dimensions and the horizontal gradients of electron density associated with them.

Fluctuations of considerable rapidity and depth have been observed at HF and VHF [1, 4, 18]. In the consideration of this problem at millimeter wavelengths it is convenient to employ the concept of a phase-changing screen [19, 20]. This screen should be envisioned as a very thin sheet across whose earthward surface are present phase variations identical to those across the bottom of an ionospheric region containing irregular "blobs" of electron density. Though near the screen only phase variations are observed, amplitude variations develop as the distance from the screen increases.

In order to anticipate the presence of scintillation, a procedure outlined by Lawrence, et al., [4] may be invoked. It has been shown that fluctuations will occur if phase variations of about one radian take place over a distance comparable to the radius of the first Fresnel zone. The Fresnel zone radius, r_1, is given by

$$r_1 = \sqrt{2\lambda} \tag{13}$$

where

$$z = \frac{ab}{a + b} \tag{14}$$

and a = the distance from source to screen,

b = the distance from screen to receiver.

As a first approximation, values for a and b are a = 35,600 km and

b = 400 km for vertical propagation. The Fresnel zone radius for these conditions is 18.45 m. The change in phase path through the ionization, ΔP, is

$$\Delta P = \frac{40.5}{f^2} \int_0^{\ell} N d\ell \ . \qquad (15)$$

Taking a typical value for the integral to be 10^{17} electrons/m^2 column, the change in phase path is 3.30 mm or 2.4 radians. Then for strong scintillations, a variation of 1 in 2.4, or about 41%, in electron density over a horizontal distance of 18.45 m would be necessary. Information presently available [21, 22, 23, 24, 25] indicates that values for electron density gradient fall far below this, in the range of 2% variation over one km.

Scintillations should increase with increasing zenith angle because both Fresnel zone radius and ΔP increase with the range. However, calculations for a zenith angle of approximately 80° indicate that a minimum variation in electron density of 7% over a horizontal distance of 45 meters would be required. Hence, it is concluded that ionospheric inhomogenieties will be of no consequence for propagation at the frequencies of interest.

III. DIRECTION OF EFFORT

During the next reporting period, it is intended that the characterization of the transmission channel be continued. The effects of turbulent atmosphere may be considerable at millimeter wavelengths and are to be evaluated as the next step in the process. Dispersive processess, phasefront distortion and noise sources will then be considered in order to determine their limiting effects on system performance. Based on this information, recommendations on methods, specifications, and system configuration will be made.

REFERENCES

[1] Davies, K., Ionospheric Radio Propagation, NBS Standard Monograph 80, April, 1965.

[2] Hartree, D. R., "The Propagation of Electro-Magnetic Waves in a Refracting Medium in a Magnetic Field," Proc. Cambridge Phil. Soc., 27, 1931.

[3] Millman, G. H., "Atmospheric Effects on VHF and UHF Propagation," Proc. IRE, August, 1958, pp. 1492 - 1501.

[4] Lawrence, R. S., Little, C. G., and Chivers, H. J. A., "A Survey of Ionospheric Effects Upon Earth-Space Radio Propagation," Proc. IEEE, 52, No. 4, January, 1964.

[5] Straiton, A. W., and Tolbert, C. W., "Factors Affecting Earth-Satellite Millimeter Wavelength Communications," IEEE Transactions on Microwave Theory and Techniques, MTT-11, No. 9, September, 1963.

[6] Van Vleck, J. H., and Weisskopf, V. F., "On the Shape of Collision-Broadened Lines," Rev. of Modern Physics, 17, No. 2 and 3, April-July, 1945.

[7] Van Vleck, J. H., "The Absorption of Microwaves by Oxygen," Phys. Rev., 71, No. 7, April, 1947.

[8] Falcone, V. J., Jr., "Calculations of Apparent Sky Temperature at Millimeter WAvelengths," Radio Science, 1, (New Series), No. 10, October, 1966.

[9] Altshuler, E. E., Falcone, V. J., and Wulfsberg, K. N., "Atmospheric Effects on Propagation at Millimeter Wavelengths," IEEE Spectrum, 5, No. 7, July, 1968.

[10] Wulfsberg, K. N., "Atmospheric Attenuation at Millimeter Wavelengths," Radio Science, 2, (New Series), No. 3, March, 1967.

[11] Mitchell, R. L., "Some Applications of Millimeter Waves in Atmospheric Research," IEEE WESCON Convention Record, 1964.

[12] Goldstein, H., Propagation of Short Radio Waves, McGraw-Hill, New York, 1951.

[13] Holzer, W., "Atmospheric Attenuation in Satellite Communications," Microwave Journal, 8, No. 3, March, 1965.

[14] Mie, G., "Beitruge zur Optik truber Medien, speziell kolloidale Metallosungen, Ann. der Phys., 25, March, 1908.

[15] Medhurst, R. G., "Rainfall Attenuation of Centimeter Waves: Comparison of Theory and Measurement," IEEE Transactions on Antennas and Propagation, AP-13, July, 1965.

[16] Robinson, N. P., "Measurements of the Effect of Rain, Snow, and Fogs on 8.6 mm Radar Echoes," Proc. IEE, 102, Pt. B, September, 1955.

[17] Lawrence, R. S., and Posakony, D. J., "A Digital Ray-Tracing Program for Ionospheric Research," Space Research II, Proc. 2nd Intern. Space Science Symposium, Florence, N. Holland Publishing Co., 1962.

[18] Yeh, K. C., and Swenson, G. W., Jr., "The Scintillation of Radio Signals from Satellites," Journal of Geophys. Res., 64, No. 12, December, 1959.

[19] Booker, H. G., Ratcliffe, J. A., and Shinn, D. H., "Diffraction from an Irregular Screen with Applications to Ionospheric Problems," Philos. Trans. Roy. Soc. London., Ser. A. 242, 1950.

[20] Mercier, R. P., "Diffraction by a Screen Causing Large Random Phase Fluctuations," Proc. Cambridge Philos. Soc., 58, No. 2, 1961.

[21] Bhonsle, R. V., "Diurnal Variations of Large-Scale Ionospheric Irregularities," J. Geophys. Res., 71, No. 19, October, 1966.

[22] Goodman, J. M., "Electron Content Inhomogeneities in the Lower Ionosphere," J. Geophys. Res., 72, No. 21, November, 1967.

[23] Fook, G. F., "Ionospheric Irregularities and the Phase Paths of Radio Waves," J. Atmos. and Terres. Phys., 24, 1962.

[24] Merrill, R. G., Lawrence, R. S., and Roper, N. J., "Synoptic Variations and Vertical Profiles of Large-Scale Ionospheric Irregularities," J. Geophys. Res., 68, No. 19, October, 1963.

[25] Little, C. G., and Lawrence, R. S., "The Use of Polarization Fading of Satellite Signals to Study the Electron Content and Irregularities in the Ionosphere," J. Res., N.B.S., 64D, No.4, July - August, 1960.

B. RADIO FREQUENCY SYSTEMS

FM Television Transmitter Exciter Unit Development

M. A. Honnell, W. E. Faust, and H. L. Deffebach

I. INTRODUCTION

During this reporting period, good progress was made in the construction and testing of the 2250-MHz television exciter unit. Major accomplishments were the completion of the transmitter case and the mounting and interconnection of the individual circuit modules into the case. Efforts were also directed toward (1) the testing of the dc-to-dc converter, (2) the design of the filter networks between the converter outputs and individual transmitter circuits, (3) the determination of the frequency stability of the reference oscillator and (4) the initiation of work on an instruction manual.

II. FABRICATION OF PROTOTYPE EXCITER UNIT

The major progress this quarter was made in the fabrication of the 2250-MHz prototype exciter. All of the machining operations on the case and on its associated cover plates were completed. The individual circuit boards for the exciter unit were also constructed. These circuit modules were then mounted and interconnected in the case. The photographs of Figures 9 and 10 show these modules as they are connected. A photograph of the complete transmitter is given in Figure 11.

During the next reporting period the major effort will be directed toward solving interface problems in the system and the complete testing of the transmitter.

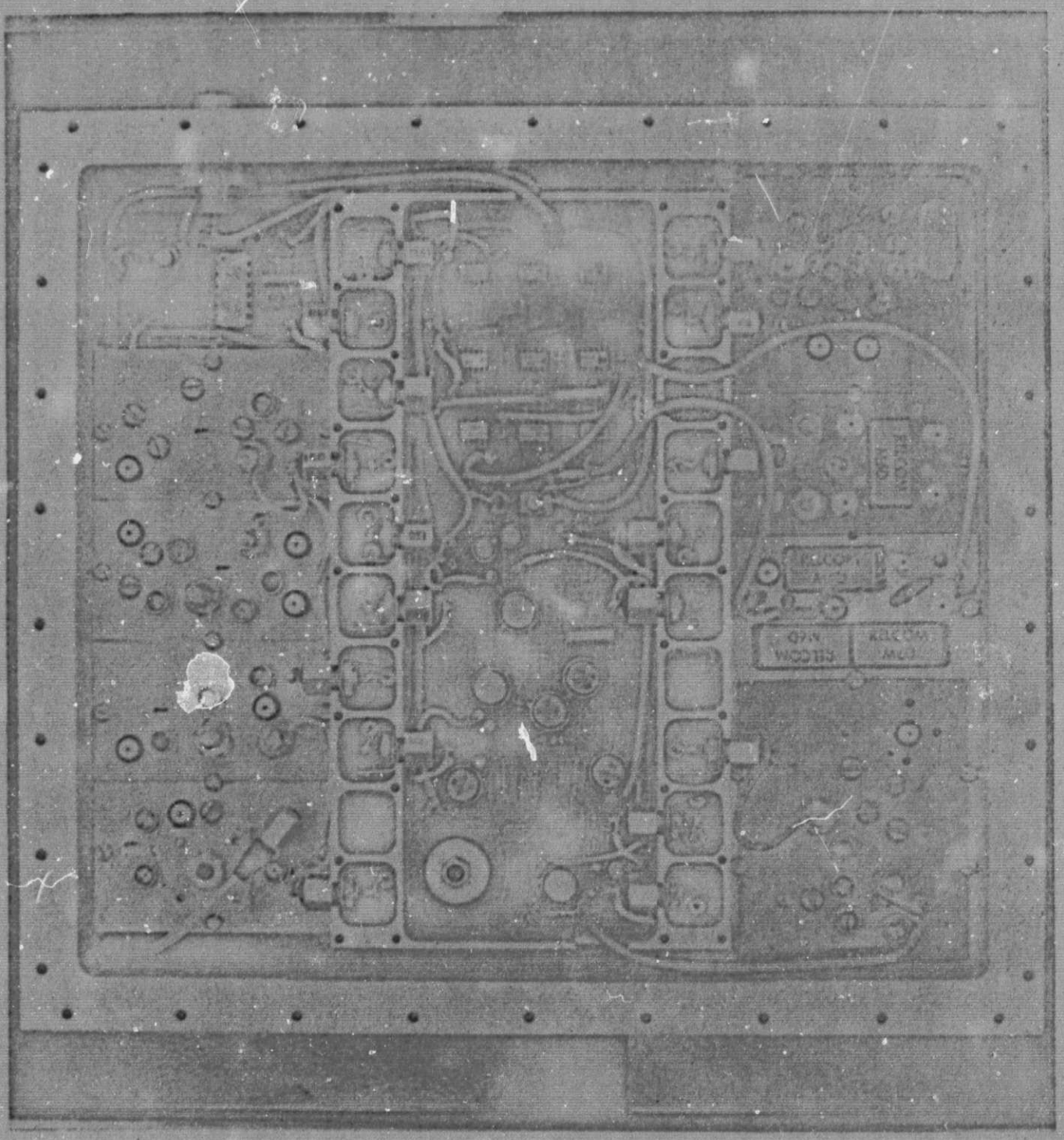

Fig. 9 -- Top View of the exciter unit.

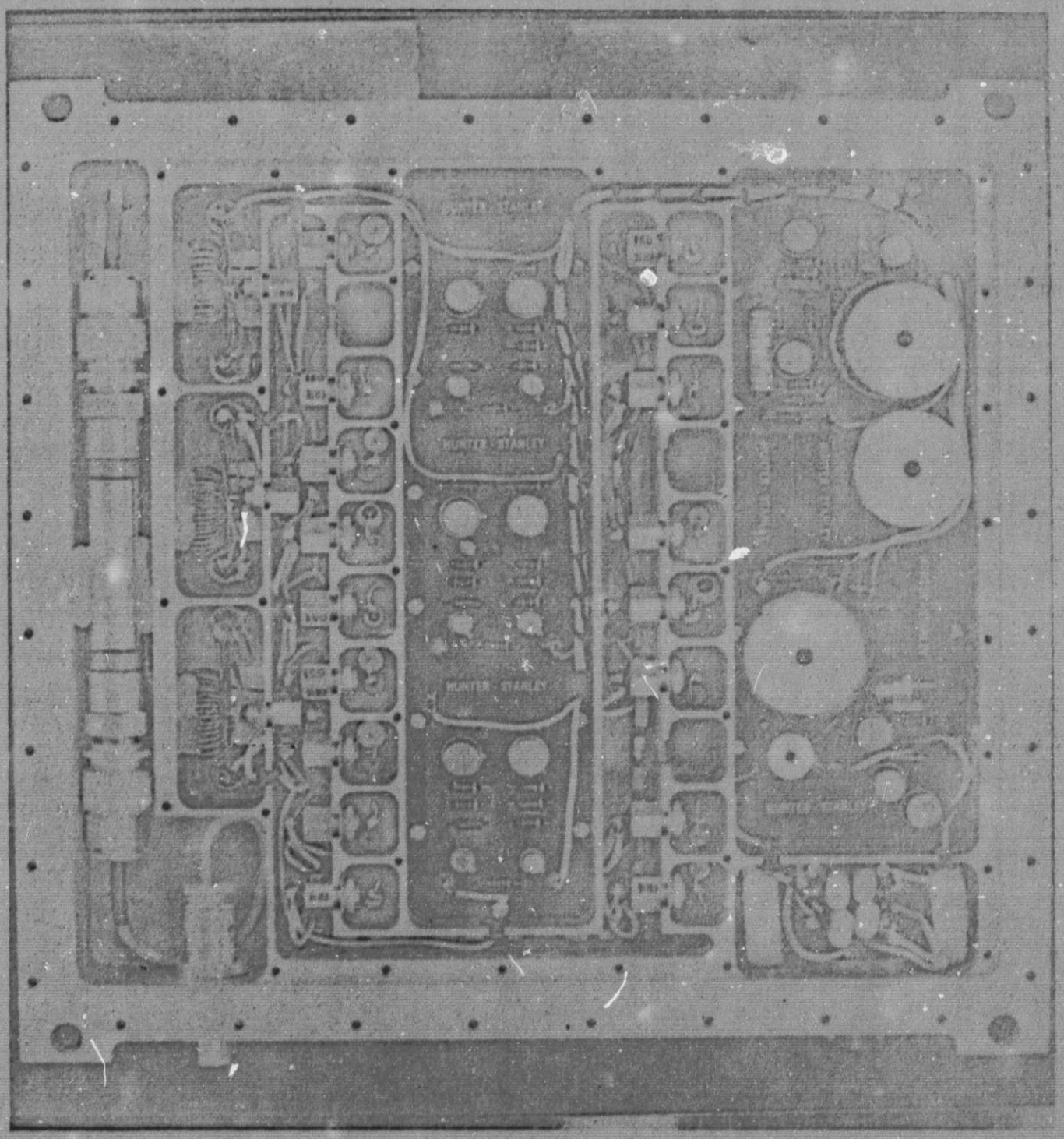

Fig. 10 -- Bottom View of the exciter unit.

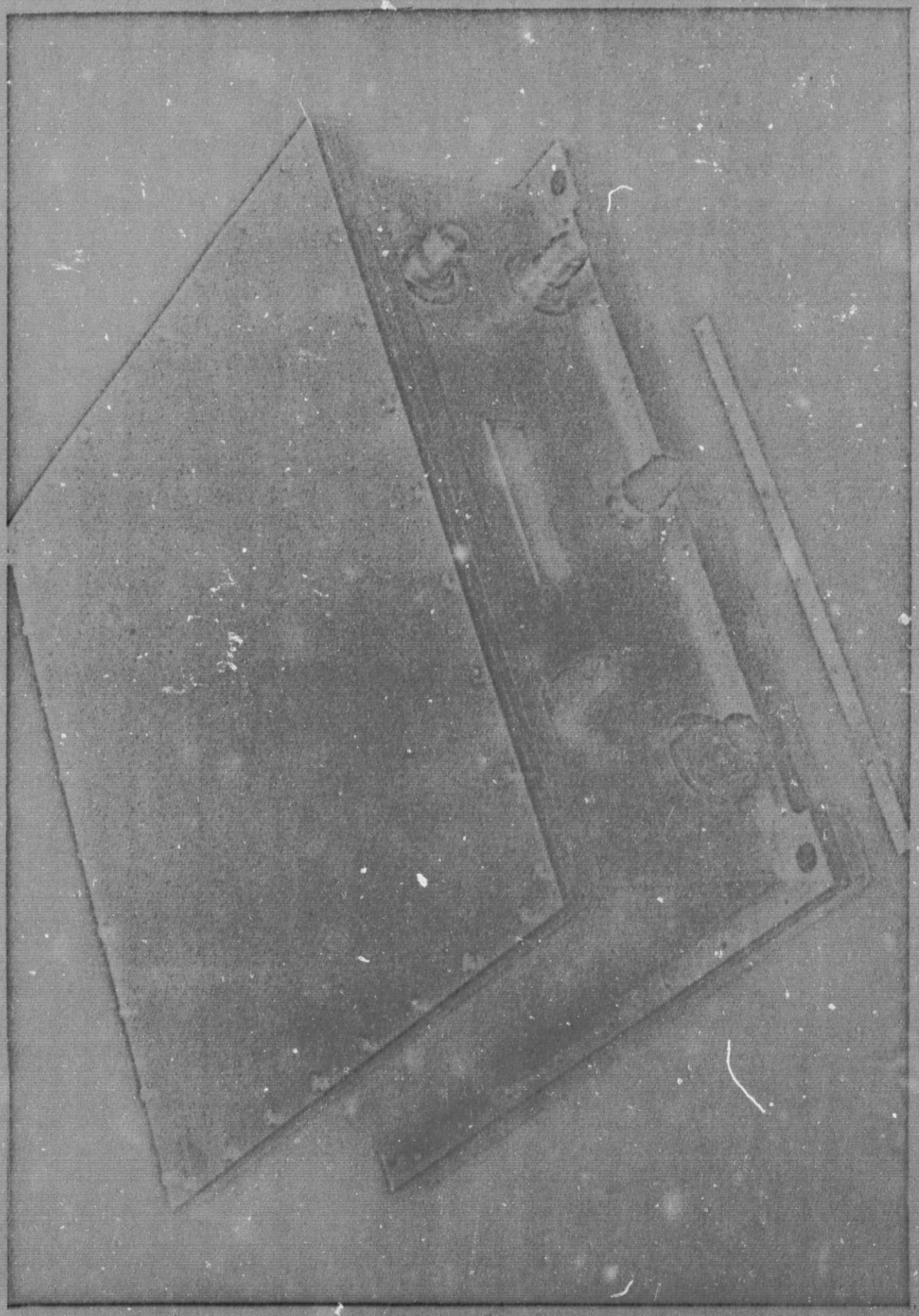

Fig. 11 — Photograph of the complete 2250-MHz FM television exciter unit.

III. FREQUENCY STABILITY OF REFERENCE OSCILLATOR

The crystal-controlled oscillator and buffer amplifier shown in Figure 12 will be employed as the reference oscillator in the transmitter. The frequency stability of this reference source was measured for variations in temperature from minus-20 degrees to plus-80 degrees Celsius. This stability is required, as was shown in the stability analysis presented in the thirteenth quarterly report, to be at least .002 per cent. Test results on the reference oscillator, which are shown in Figure 13, indicate that it has a frequency stability of .0018 per cent for the 100-degree temperature variation.

IV. CONSTRUCTION OF DC-TO-DC CONVERTER

Construction of the redesigned dc-to-dc converter circuits that conform to requirements of the prototype case was completed and the converter was wired into the case. Operating with the shielding and filtering provided in the case, the converter-output-voltage ripple and spikes were found to be smaller than those obtained from the breadboard converter model.

Additional filtering was added between each individual circuit board of the exciter and the voltage outputs of the converter. These filters are designed to provide the isolation required by the high-gain circuits in the AFC portion of the exciter unit.

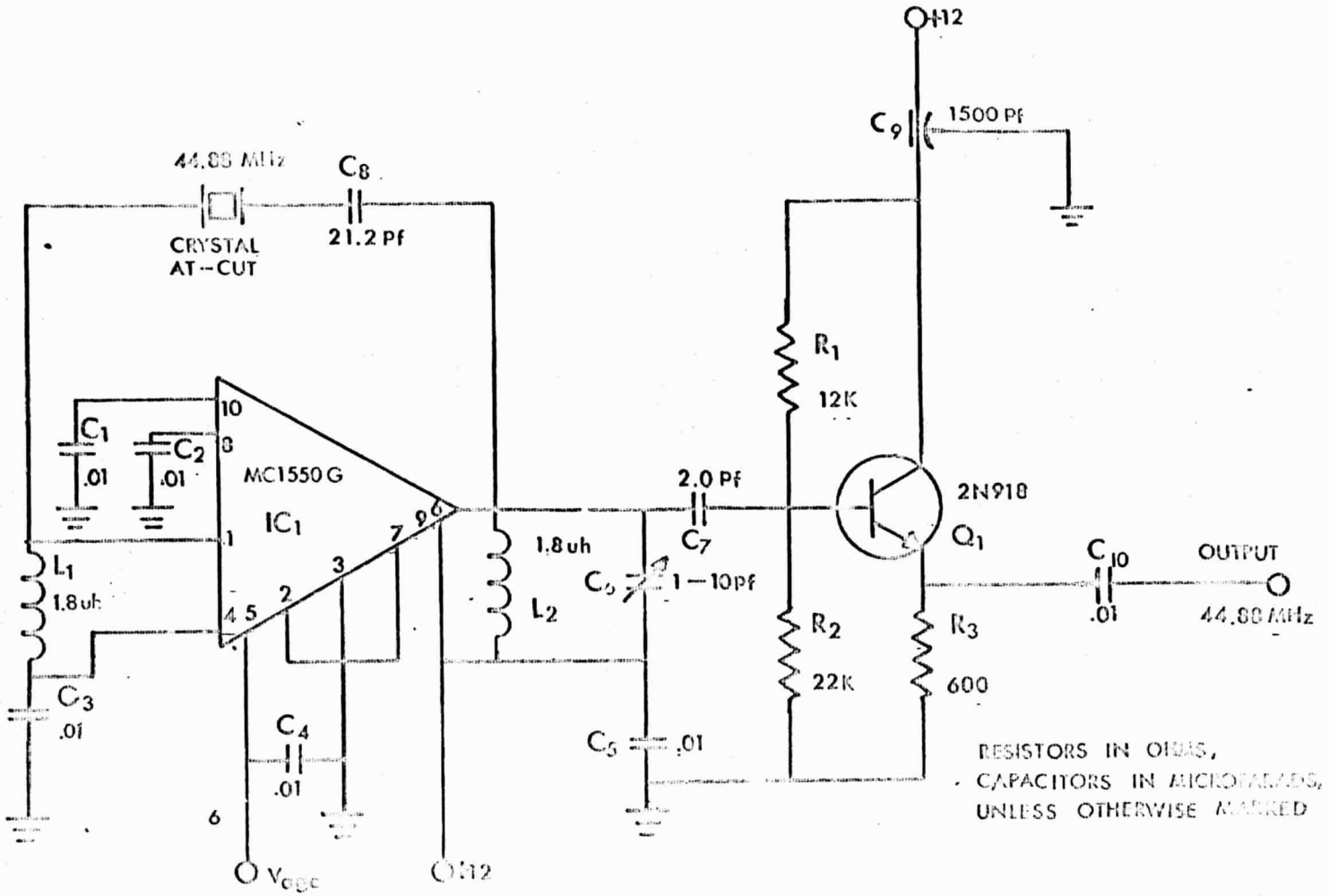

Fig. 12 — Circuit diagram of the reference oscillator.

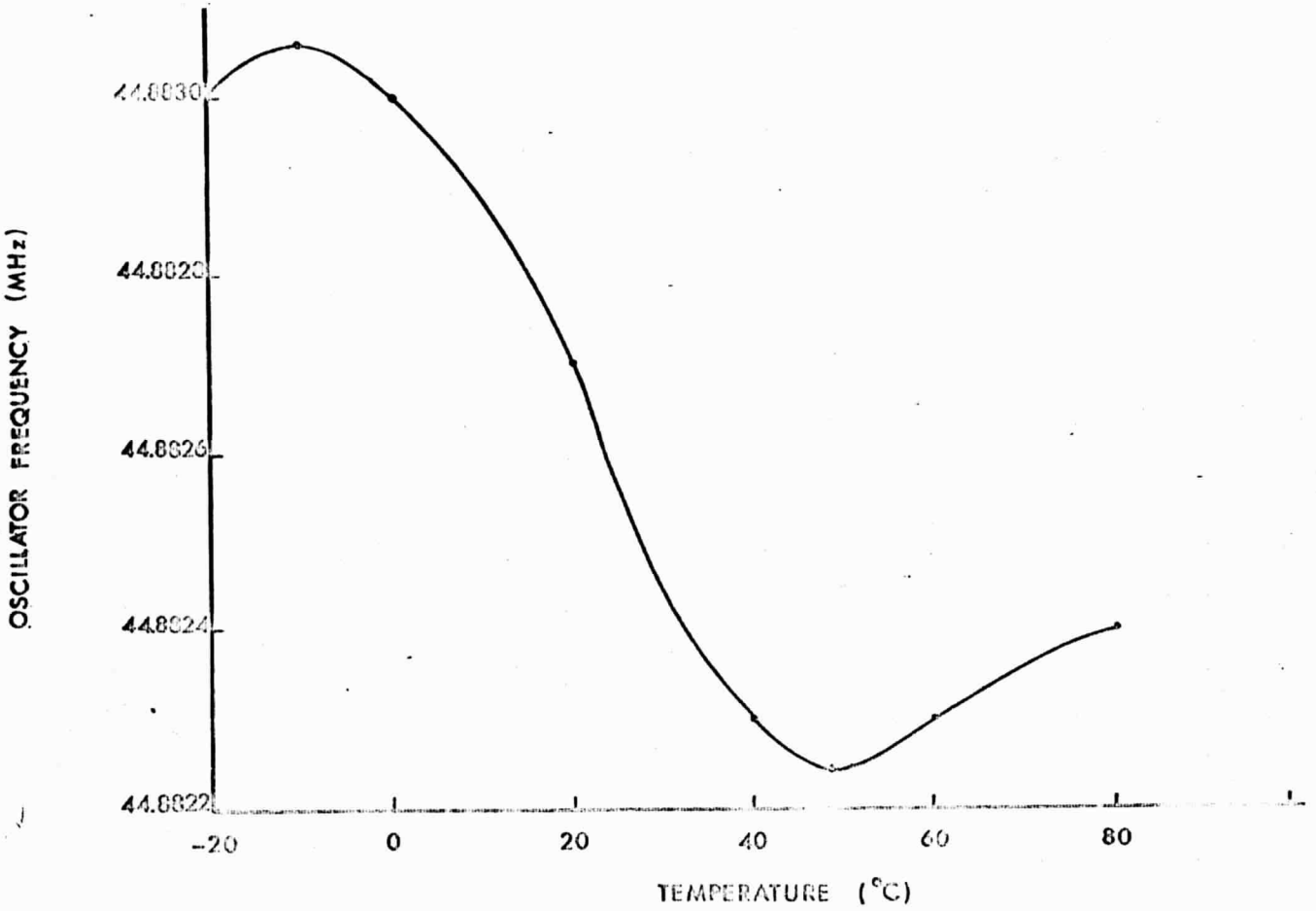

Fig. 13 — A graph of the frequency variation with respect to temperature of the reference oscillator.

V. TRANSMITTER INSTRUCTION MANUAL AND CONSTRUCTION DOCUMENTATION

Work on preparation of an instruction manual for the exciter unit was initiated. This manual will include schematic diagrams, parts list, photographs, test data, theory and adjustment procedures. Along with the manual, documentation of construction procedures including transmitter case machine drawings, printed-board negatives and machine drawings for the aluminum plates required for the RF circuit modules is being prepared.